The Rotational Zeeman Effect of Pyrazole and Imidazole

M. Stolze and D. H. Sutter

Abteilung Chemische Physik im Institut für Physikalische Chemie der Universität Kiel

Z. Naturforsch. **42 a,** 49–56 (1987); received August 30, 1986

The rotational Zeeman effect of the most abundant isotopic species of pyrazole and of imidazole has been studied under $\Delta M = 0$ and $\Delta M = \pm 1$ selection rules. With field close to 1.9 Tesla, the nuclear Zeeman effect uncouples the rotational angular momentum and the spins of the two nonequivalent ^{14}N quadrupole nuclei. The observed g-tensor elements are $g_{aa} = -0.07498(14)$, $g_{bb} = -0.12531(13)$, and $g_{cc} = 0.06346(12)$ for pyrazole and $g_{aa} = -0.09339(16)$, $g_{bb} = -0.10444(14)$, and $g_{cc} = 0.06051(15)$ for imidazole. The values for the magnetic susceptibility anisotropies in units of 10^{-6} erg/(G^2 mol) are $2\chi_{aa} - \chi_{bb} - \chi_{cc} = 39.53(24)$ and $2\chi_{bb} - \chi_{cc} - \chi_{aa} = 51.20(21)$ for pyrazole and $2\chi_{aa} - \chi_{bb} - \chi_{cc} = 45.76(31)$ and $2\chi_{bb} - \chi_{cc} - \chi_{aa} = 42.19(41)$ for imidazole. (Given uncertainties are single standard deviations of the fit.)

The so-called nonlocal (π-ring current) contributions to the out of plane components of the susceptibility tensor, $\chi_{cc}^{\text{nonlocal}}$, derived as differences between the observed susceptibilities and values calculated from additivity rules for local atom susceptibilities, are compared to those derived earlier for other aromatic five membered ring molecules.

Introduction

Aromatic molecules, i.e. molecules with a planar ring system containing $(4n+2)$-π-electrons, usually show an excess of the magnetic susceptibility tensor element perpendicular to the plane of the ring if compared to related open chain molecules [1, 2, 3, 4]. Microwave rotational Zeeman spectroscopy [5, 6], by which the susceptibility anisotropies of free molecules are measured directly, is an ideal tool to study this magnetic characteristics of delocalization. In the following contribution we present the results of such a rotational Zeeman effect investigation for the low J rotational spectra of pyrazole and imidazole. We found such an investigation of special interest, since a thermodynamic comparison of these two pyrrole related aromatic rings has been reported [7], in which imidazole is assigned only about one half the resonance energy of pyrazole. Would this difference in resonance energies translate into a corresponding difference in the nonlocal contribution to the out of plane susceptibility?

Pyrazole and imidazole, both crystals at room temperatures with melting points of 70 °C and 90 °C respectively [8], were purchased from EGA-Chemie and were purified by vacuum sublimation. Where ever possible the spectra were recorded in the superheterodyne bridge spectrometer with additional 5 kHz Stark effect square wave modulation described earlier [9]. Only two Q-band transitions of imidazole, the $1_{10}-2_{11}$ transition at 32893.824 MHz and the $2_{02}-3_{03}$ transition at 33416.088 MHz, are recorded with a conventional Stark effect moduled spectrometer (30 kHz square wave modulation, compare too [10, 11]). The absorption cells of the bridge system were rectangular brass waveguide cells with central Stark electrode and an inner cross section of 34.8 mm by 15.8 mm. Their effective length was 2 m (= length of the Stark septum used for modulation). The cells used for the Q-band measurements were rectangular brass cells with an inner setion of 45.7 mm by 10.2 mm and an effective length of 1.8 m. Sample pressures ranged between 0.2 Pa and 0.5 Pa (1.5 and 3.8 mTorr) at cell temperatures of −35 °C (pyrazole) and +20 °C (imidazole). To get signal to noise ratios of at least 10:1, digital signal averaging was used throughout (FABRITEK instrument computer model 1072). Typical line widths were 25 kHz to 60 kHz half width at half height. In order to record the Zeeman spectra, the absorption cells were loaded into the gap of a specially designed electromagnet [12, 13], which was operated at a field of approximately 19 kG (1.9 Tesla) at a gap width of 5 cm. In Fig. 1 we demonstrate the typical quality of the observed multiplet patterns. It shows the zero

---

Reprint requests to Prof. Dr. D. H. Sutter, Institut für Physikalische Chemie der Universität Kiel, Olshausenstr. 40–60, D-2300 Kiel, West Germany.

0340-4811 / 87 / 0100-0049 $ 01.30/0. – Please order a reprint rather than making your own copy.

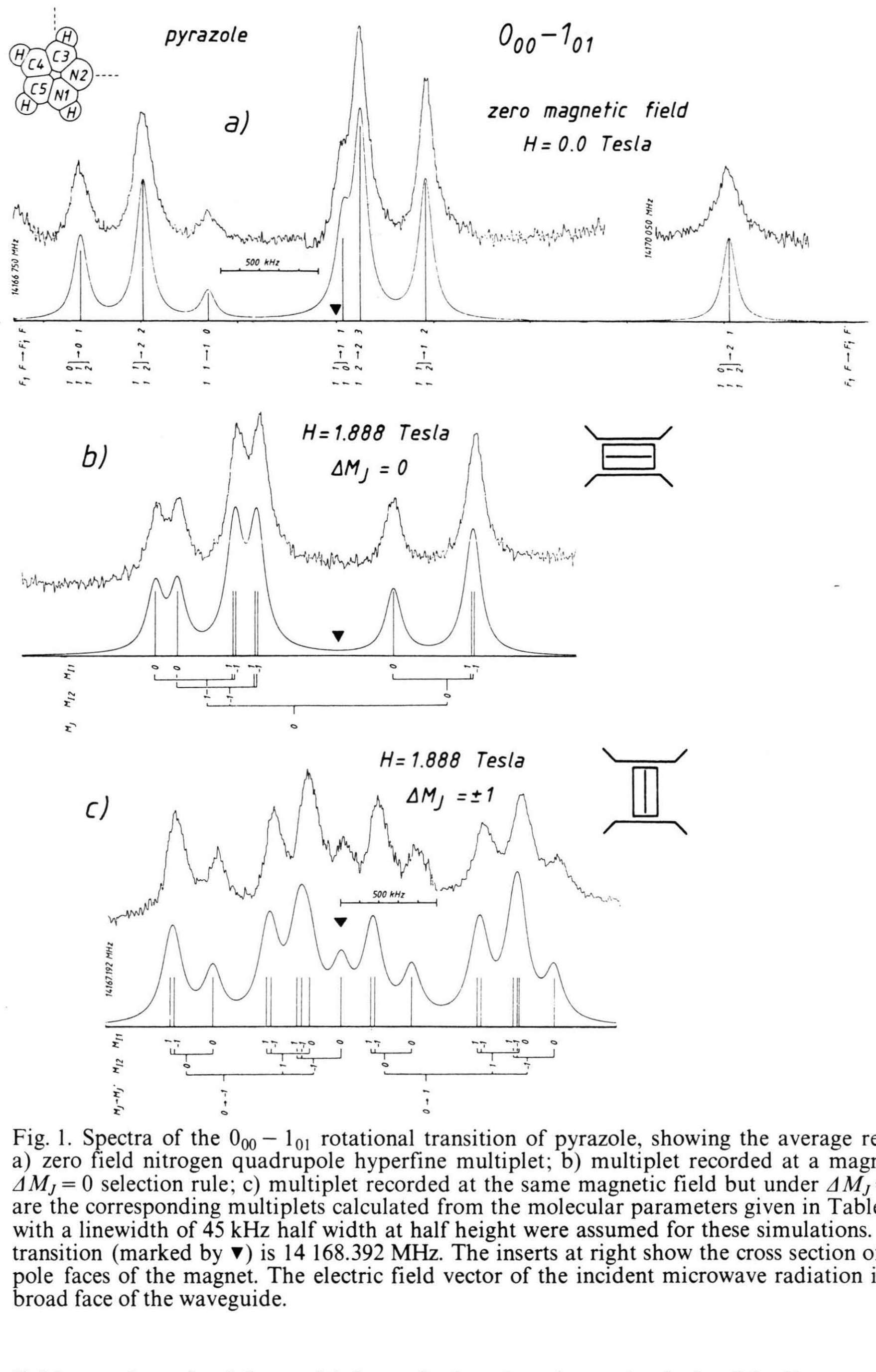

Fig. 1. Spectra of the $0_{00} - 1_{01}$ rotational transition of pyrazole, showing the average resolution obtained in this study; a) zero field nitrogen quadrupole hyperfine multiplet; b) multiplet recorded at a magnetic field of 1.8878 Tesla under $\Delta M_J = 0$ selection rule; c) multiplet recorded at the same magnetic field but under $\Delta M_J = \pm 1$ selection rule. Also shown are the corresponding multiplets calculated from the molecular parameters given in Tables 3 and 4. Lorentzian lineshapes with a linewidth of 45 kHz half width at half height were assumed for these simulations. The rigid rotor frequency of the transition (marked by ▼) is 14 168.392 MHz. The inserts at right show the cross section of the waveguide cell between the pole faces of the magnet. The electric field vector of the incident microwave radiation is polarized perpendicular to the broad face of the waveguide.

field quadrupole hfs multiplet of the $0_{00}-1_{01}$ rotational transition of pyrazole as well as the corresponding Zeeman multiplets observed under $\Delta M_J = 0$ (electric vector of the microwave field parallel to the magnetic field vector) and $\Delta M_J = \pm 1$ selection rule (microwave field polarized perpendicular to the magnetic field).

Analysis of the Spectra

a) Zero Field Spetra

The zero field microwave spectra of pyrazole and imidazole are well known [14, 15, 16, 17, 18]. These earlier studies have lead to the knowledge of the structures, the ^{14}N quadrupole coupling tensors of

Table 1. Zero field ^{14}N quadrupole hfs multiplets observed for pyrazole. We have also analysed the following transitions: $0_{00}-1_{11}$, $2_{02}-2_{11}$, $2_{12}-2_{21}$, $3_{22}-3_{21}$, $3_{12}-3_{21}$, and $3_{22}-3_{31}$. The complete frequencies listings are available upon request (see text).

$J_{K_- K_+} - J'_{K'_- K'_+}$ ν_{center} (MHz)	$\nu_{obs.}$ (MHz)	$(\nu-\nu_c)_{exp.}$ (kHz)	F_1	F	F'_1	F'	$(\nu-\nu_c)_{calc.}$ (kHz)	exp. − calc. (kHz)
$0_{00}-1_{01}$	14167.097	− 1295.	1	0	0	1	− 1297.	2.
			1	1	0	1		
14 168.392(6) MHz			1	2	0	1		
	14167.419	− 973.	1	1	2	2	− 978.	5.
			1	2	2	2		
	14 167.745	− 647.	1	1	1	0	− 642.	− 5.
	14 168.525	133.	1	2	2	3	128.	5.
	14 168.864	472.	1	1	1	2	464.	8.
			1	2	1	2		
	14 170.497	2015.	1	0	2	1	2028.	− 13.
			1	1	2	1		
			1	2	2	1		
$2_{12}-2_{11}$	13 968.146	− 1862.	2	3	2	2	− 1859.	− 3.
	13 968.257	− 1751.	2	2	2	2	− 1750.	− 1.
13 970.008(9) MHz	13 968.444	− 1564.	2	3	3	3	− 1565.	1.
			2	1	2	1		
	13 968.552	− 1456.	2	2	3	3	− 1459.	3.
	13 969.046	− 962.	3	2	2	2	− 965.	3.
	13 969.128	− 880.	2	3	2	3	− 886.	6.
	13 969.385	− 623.	3	4	3	3	− 607.	− 16.
			3	2	2	1		
	13 969.641	− 367.	3	3	3	3	− 370.	3.
	13 969.758	− 250.	2	3	1	2	− 258.	8.
	13 969.851	− 157.	1	1	2	2	− 162.	5.
			2	2	1	2		
	13 970.001	− 7.	1	2	3	3	− 10.	3.
			2	2	1	1		
	13 970.079*	71.	1	2	2	1	73.	− 2.
	13 970.220	212.	1	1	2	1	204.	8.
	13 970.336	328.	3	3	2	3	313.	15.
	13 970.522	514.	3	4	3	4	502.	12.
	13 970.958	950.	3	2	3	2	958.	− 8.
	13 971.294	1286.	1	0	1	1	1276.	10.
			3	3	3	2		
			1	2	1	2		
	13 971.425	1417.	1	1	1	2	1428.	− 11.
			1	2	1	1		
	13 972.089*	2081.	1	1	1	0	2084.	− 3.

the two nitrogen nuclei, the electric dipole moment components, and, from transitions involving states with higher values of the rotational angular momentum J, to centrifugal distortion analyses for the two molecules.

In view of the fact that in the Zeeman spectra the number of satellites in each rotational transition multiplet increases rapidly with J, the present investigation was restricted to rotational transitions involving only low J rotational states with $J \leqq 3$. Eight such transitions were studied in the case of pyrazole and six in the case of imidazole. Since the knowledge of rotational constants and quadrupole coupling constants as accurate as possible is a prerequisite for the analysis of the Zeeman multiplets, we also reanalysed the zero field quadrupole hfs patterns. In Tables 1 and 2 we present our results for two rotational transitions for each molecule. The complete frequency listings are given in [19]. They have been also deposited under file number TNA7 at the Universitätsbibliothek Kiel (Westring 400, D-2300 Kiel) and may be obtained upon request. These zero field spectra were analysed with a corrected version of the program Q2SIM, provided by M. Winnewisser, Giessen, to give the rigid rotor rotational constants and the quadrupole coupling listed in Table 3. In Q2SIM the following coupling scheme is used to set up the matrix of the

Table 2. Zero field ^{14}N quadrupole hfs multiplets observed for imidazole. We have also analysed the quadrupole hyperfine structure in the following low J transitions: $2_{02}-2_{21}$, $3_{12}-3_{31}$, $3_{22}-3_{21}$, and $2_{02}-3_{03}$. As in the case for pyrazole, the complete frequency listings are available upon request.

$J_{K_- K_+} - J'_{K'_- K'_+}$ ν_{center} (MHz)	$\nu_{\text{obs.}}$ (MHz)	$(\nu-\nu_c)_{\text{exp.}}$ (kHz)	F_1	F	F'_1	F'	$(\nu-\nu_c)_{\text{calc.}}$ (kHz)	exp. − calc. (kHz)
$0_{00}-1_{01}$	14 144.643	− 1270.	1	0	0	1	− 1269.	− 1.
			1	1	0	1		
14 145.913(3) MHz			1	2	0	1		
	14 144.931	− 982.	1	1	2	2	− 983.	1.
			1	2	2	2		
	14 145.231	− 682.	1	1	1	0	− 675.	− 7.
	14 146.051	138.	1	2	2	3	135.	3.
	14 146.357	444.	1	1	1	2	443.	1.
			1	2	1	2		
	14 147.947	2034.	1	0	2	1	2031.	3.
			1	1	2	1		
			1	2	2	1		
$1_{10}-2_{11}$	32 891.720	− 2104.	0	1	2	2	− 2104.	0.
	32 891.987	− 1837.	0	1	2	1	− 1834.	− 3.
32 893.824(8) MHz	32 892.590*	− 1234.	2	2	2	2	− 1251.	17.
	32 892.771	− 1053.	0	1	1	2	− 1052.	− 1.
			0	1	1	1		
			2	2	3	3		
	32 893.144	− 680.	2	3	2	2	− 672.	− 8.
			0	1	1	0		
			2	2	2	3		
			2	1	2	2		
	32 893.353	− 471.	2	3	3	3	− 464.	− 7.
	32 893.708*	− 116.	2	3	2	3	− 109.	− 7.
	32 894.025	201.	2	3	3	4	201.	0.
			1	2	3	3		
	32 894.368	544.	2	1	3	2	544.	0.
			1	2	2	3		
	32 894.834	1019.	1	2	1	2	1009.	10.
	32 895.559	1735.	1	1	1	2	1722.	13.
			1	1	1	1		
	32 895.907	2083.	1	1	1	0	2100.	− 17.

Hamiltonian. First the rotational angular momentum, $\boldsymbol{J}$, is coupled to the spin of the first quadrupole nucleus, the pyrrolic ^{14}N nucleus in our case, to give an intermediate angular momentum, $\boldsymbol{F}_1$. Second, this intermediate angular momentum is coupled to the spin of the second quadrupole nucleus, the pyridinic nitrogen nucleus in our case, to give the final angular momentum, $\boldsymbol{F}$. The matrix of the effective rotational Hamiltonian is set up in this coupled basis and is diagonalized numerically, Since matrix elements which are off diagonal in the rotational state quantum numbers $J, K_- K_+$ are neglected, which leads to smaller submatrices to be diagonalized, the resulting energies are only approximate. In the case of nitrogen nuclei, where the neglected matrixelements are on the order of 1 MHz, while the differences in the connected diagonal elements are typically on the order of GHz, this approximation is feasible.

This coupling scheme: $\boldsymbol{J}+\boldsymbol{I}_1=\boldsymbol{F}_1$, $\boldsymbol{F}_1+\boldsymbol{I}_2=\boldsymbol{F}$, is also used to label the hfs satellites in Fig. 1. The zero field spectrum can be directly compared to Fig. 1, trace b, of [15]. The reader is reminded however, that in [15] a different coupling scheme was used by the authors. They first coupled the two nitrogen spins to give an intermediate (spin-) angular momentum, $\boldsymbol{I}_{12}$, which was then coupled to the rotational angular momentum, $\boldsymbol{J}$ to give the final angular momentum, $\boldsymbol{F}$. Thus their labelling of the satellites differs from ours.

As expected, the superior resolution of the superheterodyne bridge spectrometer lead to considerably reduced experimental uncertainties for the quadrupole coupling constants.

Table 3. Rotational constants and nuclear quadrupole coupling constants of pyrazole and imidazole, fitted to the zero field frequencies and splittings of eight rotational transitions of pyrazole and of six rotational transitions of imidazole respectively. The index (1) refers to the pyrrolic nitrogen nucleus. The index (2) refers to the pyridinic nitrogen nucleus. Uncertainties (in brackets) are single standard deviations of the least squares fit and are given in units of the least significant digit.

	Pyrazole	Imidazole
A/MHz	9618.762(18)	9725.272(11)
B/MHz	9412.521(18)	9373.959(11)
C/MHz	4755.867(18)	4771.919(8)
$\chi_{aa}^{\mathrm{N}}(1)$/MHz	1.391(6)	1.281(7)
$\chi_{bb}^{\mathrm{N}}(1)$/MHz	1.662(6)	1.278(7)
$\chi_{aa}^{\mathrm{N}}(2)$/MHz	– 3.960(5)	– 3.981(5)
$\chi_{bb}^{\mathrm{N}}(2)$/MHz	3.140(5)	1.753(8)

Table 4. Zeeman parameters of pyrazole and imidazole from a least squares fit to 123 experimental satellite frequencies of 8 rotational transitions in the case of pyrazole and of 77 satellite frequencies of 6 rotational transitions in the case of imidazole. Only the relative sign of the g values can be determined from a high field Zeeman study as reported here [24]. In our case however, the choice with opposite signs can be discarded, since it would lead to unresonable values for the components of the molecular electric quadrupole moment tensor and to a negative value for the out of plane second moment of the electron charge distribution, $\langle 0|\sum_i^{\text{electrons}} c_i^2|0\rangle$.

	Pyrazole	Imidazole
g_{aa}	– 0.07498(14)	−0.09339(16)
g_{bb}	– 0.12531(13)	−0.10444(14)
g_{cc}	0.06346(12)	0.06051(15)
$2\chi_{aa}-\chi_{bb}-\chi_{cc}$ /10^{-6} erg G^{-2} mol^{-1}	39.53(24)	45.76(31)
$2\chi_{bb}-\chi_{cc}-\chi_{aa}$ /10^{-6} erg G^{-2} mol^{-1}	51.20(21)	42.19(41)

Table 5. Molecular electric quadrupole moments and electronic ground state expectation values for the anisotropies in the second moments of the electron charge distribution of pyrazole and imidazole, all referred to the principal inertia axes systems, i.e. center of mass systems. The equations used to calculate the quadrupole moments and anisotropies are:

$$Q_{aa}=-\frac{\hbar e}{8\pi m_{\mathrm{p}}}\left\{\frac{2g_{aa}}{A}-\frac{g_{bb}}{B}-\frac{g_{cc}}{C}\right\}-\frac{2mc^2}{e}\{2\chi_{aa}-\chi_{bb}-\chi_{cc}\},$$

$$\langle 0|\sum_i^{\text{electrons}}(b_\varepsilon^2-c_\varepsilon^2)|0\rangle=\sum_v^{\text{nuclei}}Z_v(b_v^2-c_v^2)+\frac{h}{8\pi^2 m_{\mathrm{p}}}\left(\frac{g_{bb}}{B}-\frac{g_{cc}}{C}\right)+\frac{4mc^2}{3e^2}\{(2\chi_{bb}-\chi_{aa}-\chi_{cc})-(2\chi_{cc}-\chi_{aa}-\chi_{bb})\}.$$

(and cyclic permutations).

	Pyrazole	Imidazole
$Q_{aa}/10^{-26}$ esu cm^2	– 3.55(22)	– 0.92(27)
$Q_{bb}/10^{-26}$ esu cm^2	9.79(20)	6.79(33)
$Q_{cc}/10^{-26}$ esu cm^2	– 6.24(35)	– 5.87(53)
$\langle a^2-b^2\rangle/\text{Å}^2$	0.523(84)	– 0.154(94)
$\langle b^2-c^2\rangle/\text{Å}^2$	29.756(114)	29.976(134)
$\langle c^2-a^2\rangle/\text{Å}^2$	– 30.279(115)	– 29.822(126)

B) Zeeman Spectra

All Zeeman spectra were recorded at fields in the range between 18.8 and 18.9 kG. Just as in the case of pyrrole [20], pyridine [21], and the fluorine substituted pyridines [22, 23], the nuclear Zeeman effect quite effectively uncouples molecular rotation and the spins of the quadrupole nuclei ^{14}N. Thus the uncoupled basis, $|J, K_- K_+, M_J\rangle$, $|I_1, M_1\rangle$, $|I_2, M_2\rangle$, already gives good first order energies and was used to set up the matrix of the effective Hamiltonian. Again, as in the zero field case, the matrixelements off diagonal in $J, K_- K_+$ were neglected.

For improved approximation of the Zeeman energies of the different rotational states, the corresponding M_J, M_1, M_2-submatrices, they are of rank $(2J+1)$ $(2I_1+1)$ $(2I_2+1)$, were subjected to a third order perturbation treatment. This leads to kHz accuracy of the energies, well below our experimental resolution.

Due to the very effective uncoupling of the spins, the observed Zeeman multiplets correspond to transitions, which obey $\Delta M_1=0$ and $\Delta M_2=0$ selection rules for the spins, and, depending on the orientation of the microwave electric field vector with respect to the magnetic field axis, $\Delta M_J=0$ or $\Delta M_J=\pm 1$ selection rules for the projection of the rotational angular momentum J on the magnetic field axis. For a demonstration of the change in the selection rules when proceeding from the coupled case at low fields to the uncoupled case at fields above approximately 10 kG, the reader is referred to Fig. 5 in [24]. For details of the theory of the rotational Zeeman effect of molecules containing nuclei with nuclear quadrupole coupling and for the matrixelements of the effective Hamiltonian we refer to [12] and [6], Eqs. (III,9) through (III,13), (III,20) through (III,24) and Chapter IV.

In the case of pyrazole and imidazole, the Zeeman multiplets corresponding to a specific rotational transition typically stretch over a frequency range of ± 3.5 MHz. Due to the many satellites in such a multiplet, it was not possible to resolve them all as isolated lines, even not with the high resolution power of the superhet bridge system. Thus, in the fit of the g-values and susceptibility anisotropies, we used only the well resolved satellites and some selected features in the spetra, where the frequency of the observed "lines" could be approximated as the intensity weighted means of the overlapping satellites [25].

In our assignment of the Zeeman satellites we started out from susceptibility anisotropies predicted from local increments [26, 27] and a nonlocal (π-ring current contribution) estimated from pyrrole [20]. Analysis of the $J = 0$ to $J = 1$ Zeeman spectra, observed under $\Delta M_J = 0$ selection rule, which, apart from ^{14}N quadrupole hfs, predominantly depend on the susceptibility anisotropies, then lead to improved susceptibility anisotropies. In the next step initial g tensor elements could be calculated from the susceptibilities, the known structures, and from second moments of the electron charge distribution obtained from a CNDO/2 calculation [28]. With these approximate g values Zeeman spectra could be predicted, which came sufficiently close to the observed patterns in order to make an assignment possible. In all, 123 frequencies were used to fit the g values and susceptibility anisotropies of pyrazole, and 77 frequencies were used to fit the corresponding values of imidazole. The Zeeman multiplet listings are again deposited under file number TNA7 at the Universitätsbibliothek Kiel and are available upon request. In Table 4 we present the results of the least squares fit.

With the Zeeman parameters listed in Table 4 and the theoretical treatment described above, the observed multiplet patterns are reproduced typically within better than 10 kHz.

Table 6. Comparison of the nonlocal out of plane (π-ring current) contribution, $\chi_{cc}^{\text{nonlocal}}$, of the magnetic susceptibility tensor for some aromatic 5-membered ring molecules.

		$\chi_{cc}^{\text{nonlocal}}$ $/10^{-6}\,\text{erg}\,\text{G}^{-2}\,\text{mol}^{-1}$	Ref.
furane	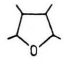	- 24.0	(35)
isoxazole	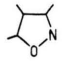	- 26.0	(36)
oxazole	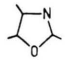	- 22.5	(36)
pyrrole	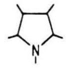	- 31.9	(20)
pyrazole	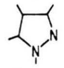	- 33.3	this work
imidazole	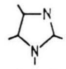	- 34.7	this work
thiophene	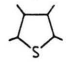	- 36.4	(35)
isothiazole	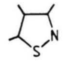	- 37.2	(27)
thiazole	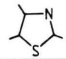	- 39.5	(27)

From the known structures [16, 17], and from the theoretical expressions for the rotational constants and for the g- and χ-tensor elements [29], the experimental rotational constants, g-values and susceptibility anisotropies can be used to derive "experimental" vibronic ground state expectation values for the components of the molecular electric quadrupole moment tensor and for the anisotropies in the second moments of the electron charge distribution [30, 31]. These values are given in Table 5. The reader is reminded that the values are referred to the principal inertia axes systems of the two molecules. In both molecules the molecular electric quadrupole moment tensor for instance certainly has a nonvanishing off diagonal element Q_{ab}, if referred to this axis system. However pyrazole and imidazole are both molecules which, as far as their moments of intertia are concerned, come very close to the limiting case of an oblate symmetric top, and isotopic substitutions lead to considerable changes of the orientation of the a- and b-axes of the principal inertia system with respect to the nuclear frame without affecting the electron distribution appreciably. Thus the Zeeman study of deuterated species should lead to the knowledge of the complete molecular electric quadrupole tensor as well as the knowledge of the complete molecular susceptibility tensor for the two molecules. Such a study is currently under way at our laboratory.

Discussion

We restrict our discussion to the nonlocal out of plane component of the susceptibility tensor. We calculate it from the experimental out of plane minus average in plane susceptibility and from the corresponding local susceptibility anisotropy as [32]:

$$\chi_{cc}^{\text{nonlocal}} := \{\chi_{cc} - (\chi_{aa} + \chi_{bb})/2\}_{\text{exp}} - \{\chi_{cc}^{\text{local}} - (\chi_{cc}^{\text{local}} + \chi_{bb}^{\text{local}})/2\}_{\text{calc}} .$$

The local susceptibilities were calculated as sums of the corresponding atomic contributions from Table 6, ref. [27]. When proceeding like this, we assume that essentially no nonlocal contribution is present in the χ_{aa} and χ_{bb} elements, an assumption which of cause holds only as an approximation [33, 34]. We note that the so calculated $\chi_{cc}^{\text{nonlocal}}$ is invariant under rotations about the *c*-axis and its evaluation does not require the knowledge of an experimental value for the bulk susceptibility. As indicated already in the introduction, its value has been proposed as a measure for "aromaticity". We therefore present a comparison of the $\chi_{cc}^{\text{nonlocal}}$ values for a group of five membered rings in Table 6. This Table shows, that the nonlocal out of plane susceptibility is nearly unaffeted by exchange of a $\geqslant$C−H group against the isoelectronic nitrogen atom. The Table also shows a grouping into three families: furane and its derivatives with values around − 24 units, pyrrole and its derivatives with values around − 33 units, and thiophene and its derivatives with values around − 38 units. We note that the same ordering of the molecules would have been obtained from their relative chemical reactivity in electrophilic substitution reactions which is a classical criterium for "aromaticity". Finally we note that the magnetic criterium for delocalization shows very little differences between pyrazole and imidazole, quite in contrast to their difference in resonance energies reported earlier based on thermodynamic studies [7], 14.2 kcal/mol for imidazole and 29.3 kcal/mol for pyrazole.

Acknowledgements

The support from Deutsche Forschungsgemeinschaft and Fonds der Chemischen Industrie is gratefully acknowledged. We also would like to thank Prof. H. Dreizler for critically reading the manuscript. All computer calculations for analysis and prediction of the spectra were performed on the PDP 10 system of the Rechenzentrum der Universität Kiel.

[1] L. Salem, The Molecular Orbital Theory of Conjugated Systems. W. A. Benjamin, New York 1966, Chapter 4.
[2] R. C. Benson, C. L. Norris, W. H. Flygare, and P. A. Beak, J. Amer. Chem. Soc. **93**, 5591 (1971), and references cited therein.
[3] T. G. Schmalz, C. L. Norris, and W. H. Flygare, J. Amer. Chem. Soc. **95**, 7961 (1973).
[4] D. Hübner, M. Stolze, and D. H. Sutter, Z. Naturforsch. **36a**, 332 (1981), and references cited therein.
[5] W. H. Flygare and R. C. Benson, Mol. Phys. **20**, 225 (1971).
[6] D. H. Sutter and W. H. Flygare, Topics in Current Chemistry **63**, 89 (1976).
[7] A. F. Bedford, P. B. Edmondson, and C. T. Mortimer, J. Chem. Soc. **1962**, 2927.
[8] Handbook of Chemistry and Physics, 65th ed. (R. C. Weast, M. J. Astle, and W. H. Beyer, eds). CRC Press Inc., Boca Raton, Florida 1984.
[9] W. H. Stolze, M. Stolze, D. Hübner, and D. H. Sutter, Z. Naturforsch. **37a**, 1165 (1982).
[10] R. H. Hughes and E. Bright Wilson Jr., Phys. Rev. **71**, 562 (1947).
[11] U. Andresen and H. Dreizler, Z. Angew. Physik **30**, 207 (1970).
[12] D. H. Sutter, Z. Naturforsch. **26a**, 1644 (1971).
[13] See Ref. [6], Chapter III.A.
[13] William H. Kirchhoff, J. Amer. Chem. Soc. **89**, 1312 (1967).
[15] G. L. Blackman, R. D. Brown, and F. R. Burden, J. Mol. Spectr. **36**, 528 (1970).
[16] D. Christen, J. H. Griffiths, and J. Sheridan, Z. Naturforsch. **37a**, 1378 (1982).
[17] Lise Nygaard, Dines Christen, J. Tormod Nielsen, E. Jonas Pedersen, Ole Snerling, Erik Vestergaard, and G. Ole Sorensen, J. Mol. Struct. **22**, 401 (1974).
[18] G. L. Blackman, R. D. Brown, F. R. Burden, and I. R. Elsum, J. Mol. Spectr. **60**, 63 (1976).
[19] M. Stolze, Dissertation Kiel (1984).
[20] D. H. Sutter and W. H. Flygare, J. Amer. Chem. Soc. **91**, 6895 (1969).

[21] E. Hamer and D. H. Sutter, Z. Naturforsch. **31a,** 265 (1976).

[22] D. Hübner, M. Stolze, and D. H. Sutter, Z. Naturforsch. **36a,** 332 (1981).

[23] D. Hübner, M. Stolze, and D. H. Sutter, Z. Naturforsch. **37a,** 95 (1982).

[24] M. Stolze and D. H. Sutter, Z. Naturforsch. **40a,** 998 (1985).

[25] Compare [22], p. 335.

[26] Compare [6], Chapt. II.C.

[27] J. Wiese and D. H. Sutter, Z. Naturforsch. **35a,** 712 (1980), and references cited therein.

[28] E. Hamer, L. Engelbrecht, and D. H. Sutter, Z. Naturforsch. **29a,** 924 (1974).

[29] Compare for instance, Ref. [6], Eqs. (I.2) through (I.8).

[30] W. Hüttner, M.-K. Lo, and W. H. Flygare, J. Chem. Phys. **48,** 1206 (1968).

[31] Compare too Ref. [6], Eqs. (II.1) and (II.3).

[32] See Ref. [23], P. 337 through 338.

[33] D. Hübner and D. H. Sutter, Z. Naturforsch. **39a,** 55 (1984), Tab. 3.

[34] See ref. [24], pp. 1008 through 1011.

[35] D. H. Sutter and W. H. Flygare, J. Amer. Chem. Soc. **91,** 4063 (1969).

[36] J. R. Davidson, A. K. Burnham, B. Siegel, P. Beak, and W. H. Flygare, J. Amer. Chem. Soc. **96,** 7394 (1974).